

Received: 16. January 2023 / Accepted: 14 February 2023 / Published online: 16 February 2023

*milling, force, dynamics,  
in-process measurement*

Christoph Ramsauer<sup>1</sup>, David LEITNER<sup>1\*</sup>,  
Christoph HABERSOHN<sup>1</sup>, Tony SCHMITZ<sup>2</sup>,  
Kazuo YAMAZAKI<sup>3</sup>, Friedrich BLEICHER<sup>1</sup>

## **FLEXURE-BASED DYNAMOMETER FOR VECTOR-VALUED MILLING FORCE MEASUREMENT**

Variation in cutting forces with cutting parameter selection, tool geometry, and wear status plays an important role for milling process evaluation and modeling. While piezoelectric force measurement is commercially available, it is often considered a precise but expensive method. This paper presents a novel solution for vector-valued cutting force measurement. The table-mounted, flexure-based kinematics provide three degrees of freedom that are used to measure the in-process milling force vector components in the working plane by low-cost optical sensors. Based on analytical models and FEM analysis, an appropriate design was derived. The assembly and testing of the developed dynamometer are presented. A test setup based on a machining center was used for the system evaluation and the data are compared to the forces measured by a commercially available, piezoelectric cutting force dynamometer.

### **1. INTRODUCTION**

CUTTING FORCES are used for the design of tools, their geometry and recommended operating parameters as shown by Fleischer et al. in [1] and Denkena and Biermann in [2]. Brecher and Weck demonstrated the importance of forces and the resulting torque and power load on machine tools and their components in [3], while Abele et al. summarized effects on machine tool spindle units in [4]. Although there are well established models for mechanistic cutting force calculation, such as from Kienzle in [5] and applied by Denkena and Tönshoff in [6], sensing process forces while machining has been a persistent trend for decades especially for tool wear detection particular in research and development purpose, e.g., Micheletti et al. in [7], Byrne et al. in [8] and Teti et al. in [9]. Direct sensing with dedicated measurement instruments located close to the cutting process is a commonly used method as shown by Wyen and Wegener in [10]. However, providing reliable measurement of direction-

---

<sup>1</sup> IFT – Institute for Production Engineering and Photonic Technologies, TU Wien, Austria

<sup>2</sup> University of Tennessee, Department of Mechanical, Aerospace, and Biomedical Engineering, United States

<sup>3</sup> Department of Mechanical Engineering, University of California, Berkeley, United States

\* E-mail: leitner@ift.at

<http://doi.org/10.36897/jme/161234>

dependent components (i.e., in vector-valued manner) can be cost intensive. Force sensors may also be integrated in machine tool structures directly near drive housings, nuts or bearings as shown by Medyk, Kasprzak and Pyzalski in [11–12]. Alternately, indirect force calculation is possible by measuring the spindle or drive motor current or power consumption as shown in [13]. Recent progress in machine learning has established increasingly precise predictions for some applications as shown by Xu et al. in [14]. Nevertheless, sensing the force via the remote information of spindle current is sometimes considered as soft functionality and in most cases the indirect method is less accurate. To provide measurement near the cutting edge, researchers have developed force sensing systems integrated in the tooling system of lathes and even rotating tools. Recently, process monitoring was summarized by Teti et al. in [15], while Bleicher et al. focused on sensor and actuator integration in the tooling system in [16]. The transduction scheme, signal transmission and power supply are key factors that can be used to categorize these sensory tooling systems.

Several solutions for force measurement on the workpiece side have also been developed. Denkena et al. showed sensory workpieces in [17] and sensing clamping elements in [18], while Palalic et al. described force sensing platforms in [19]. Utilizing the structural dynamics of a flexure-based dynamometer, Gomez and Schmitz proposed a novel low-cost sensing device for use underneath the workpiece in [20–21]. In this context low-cost refers to an inexpensive metrology method; in this use case particularly based on optical transducers. However, this low-cost dynamometer (LCD) only has one degree of freedom in motion and therefore senses only a single axis. Hybrid manufacturing of this dynamometer is shown in [22] and stability evaluation was performed in [23].

This paper shows a method of enhancing the single-axis LCD to a system capable of sensing vector-valued cutting forces in the X and Y direction. This advances the state of the art by proving vector-valued measurement of the active force in the working plane according to DIN-standard 6584 [24]. Cutting experiments are performed to evaluate the new design.

## 2. DEVELOPMENT OF THE FLEXURE-BASED DYNAMOMETER

Based on design of Gomez and Schmitz presented in [20–23], the design of the flexure-based dynamometers was enhanced. The new design consists of a monolithic metal base body and additional sensors and electronics mounted on a baseplate. The design enables constrained, linear motion in the selected directions and its dynamic properties are used to derive forces from dynamic displacement measurements.

### 2.1. FUNCTIONAL PRINCIPLE AND MECHANICAL DESIGN

The functional principle utilizes the structural dynamics of the dynamometer and is depicted in Fig. 1. The displacement of the moving platform in the lower stiffness directions prescribed by the flexure design is measured during milling. In order to determine the dynamic force from the measured displacement, the inverted displacement-to-force frequency

response function (or receptance) is applied in the frequency domain analysis. This procedure can be described as dynamic compensation, similar to filtering approached from Rubeo and Schmitz in [25] or Korkmaz et al. in [26].

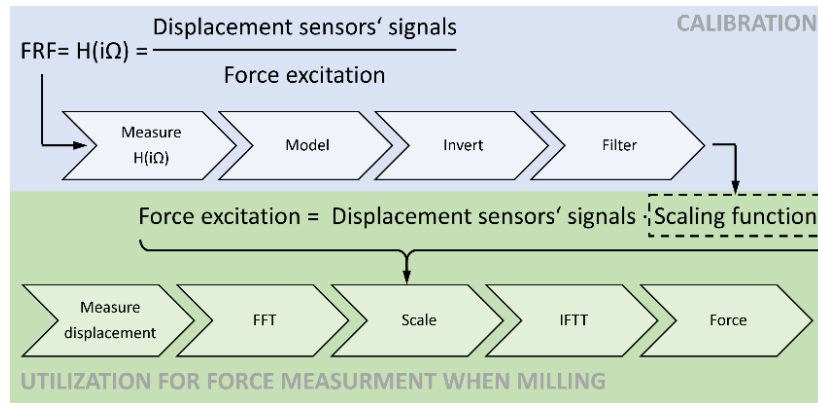


Fig. 1. Functional principle of calibrating and utilizing the structural dynamics of the dynamometer

The dynamometer is composed of a frame, flexure elements to provide constrained motion, and the moving platform, where the workpiece is mounted. The frame is stiff and provides features for mounting the dynamometer to the machine table. The thin flexure elements (i.e., flexure leaves) connect the outer frame to the inner moving platform. The dynamometer presented in this paper is made of aluminum (EN-AW-6082) and was designed to be partly wire-cut using EDM (electrical discharge machining) to create the flexure leaves with intended high bending resilience.

While the solution in [20–23] deployed single-axis force measurement and, therefore, single-axis motion of the inner platform, the new design provides motion in three possible directions: linear  $X$ , linear  $Y$  and the rotatory motion around the  $Z$ -axis (usually in line with the  $C$ -axis of a machining center). Therefore, sensing both active force components in  $X$  and  $Y$  is possible and enables vector-valued sensing of the active force. To derive the final force values, static and dynamic properties were modeled.

Table 1. Approximate values for design constraints

| Name                                      | Symbol            | Value            |
|---|-------------------|------------------|
| Maximum nominal load (in $X$ and $Y$ )    | $F_{\max}$        | 5000 N           |
| Maximum displacement (at maximum load)    | $\Delta x_{\max}$ | 80 $\mu\text{m}$ |
| Gap width for EDM                         | -                 | 1.5 mm           |
| Width of flexure leaves                   | -                 | 1.0 mm           |
| First natural frequency (in $X$ and $Y$ ) | $f$               | 1000 Hz          |

The CAD model was analyzed using finite element methods (FEM) to predict stiffness values, natural frequencies (eigenvalues), and mode shapes (eigenmodes). The parameters according to Table 1 were used to define the final design. Considerations included the sensor motion range and mass removal to increase natural frequencies, see Fig. 2.

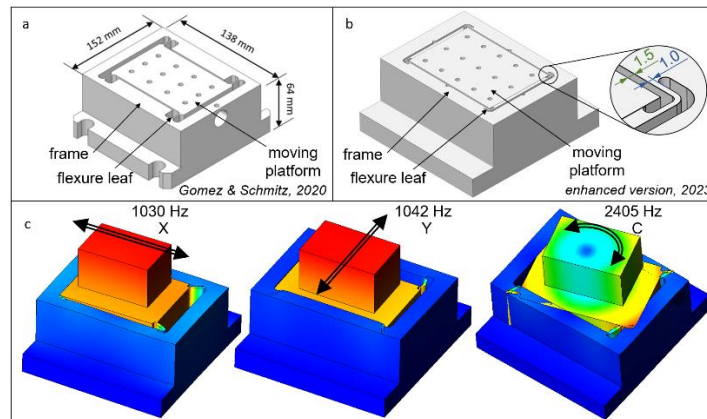


Fig. 2. Design studies and resulting eigenvalues/modes of the dynamometer

## 2.2. ELECTRICAL CONSTRUCTION AND TRANSDUCING PRINCIPLE

Properly sensing the motion of the dynamometer's moving platform was a key design issue. Several methods have been previously investigated including contactless eddy current position sensors or strain gauges mounted on the flexure elements. To provide convenient assembly, high resolution, and inexpensive and commonly available components, optical interrupters (or knife edge sensors [27]) were chosen for the final design, see Fig. 3b. The Sharp GP1S52VJ000F photointerrupter is an optical transducer that can be operated with the knife intersecting the light gap from different directions to adjust measurement range and resolution. The basic electric transducing principle is depicted in Fig. 3a. The cost of this photointerrupter is approximately 1€ per piece and the costs for the additional electronics integrated into the dynamometer sum to less than 100€.

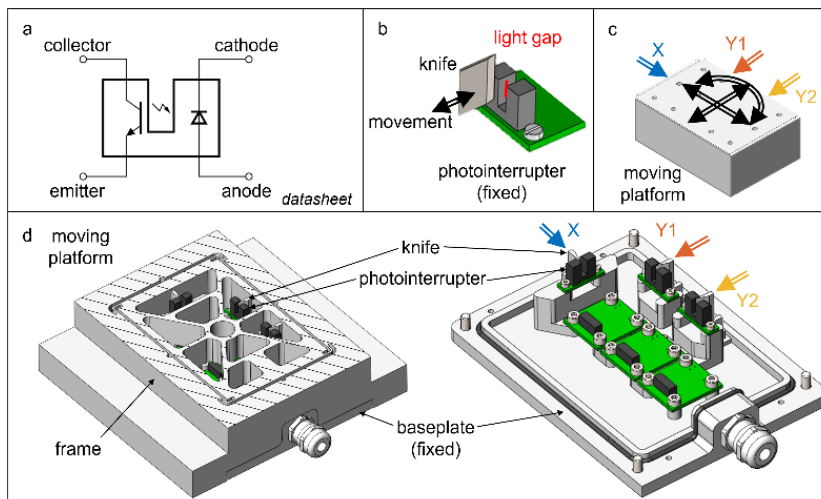


Fig. 3. Knife edge sensors used in the dynamometer

Three knife edge sensors were used to measure the motion of the moving platform as shown in Fig. 3c. The knives are mounted on the moving parts, while the optical system and

electronics are installed on the baseplate fixed to the frame as shown in Fig. 3d. The  $X$  displacement is measured with one dedicated sensor, while  $Y$  displacement and  $C$  rotation are sensed using two sensors, labeled  $Y1$  and  $Y2$ . All three sensors are aligned close to the axes of higher frequency rolling and tilting modes of the dynamometer (not shown in Fig. 2) to minimize cross-talk and measurement errors.

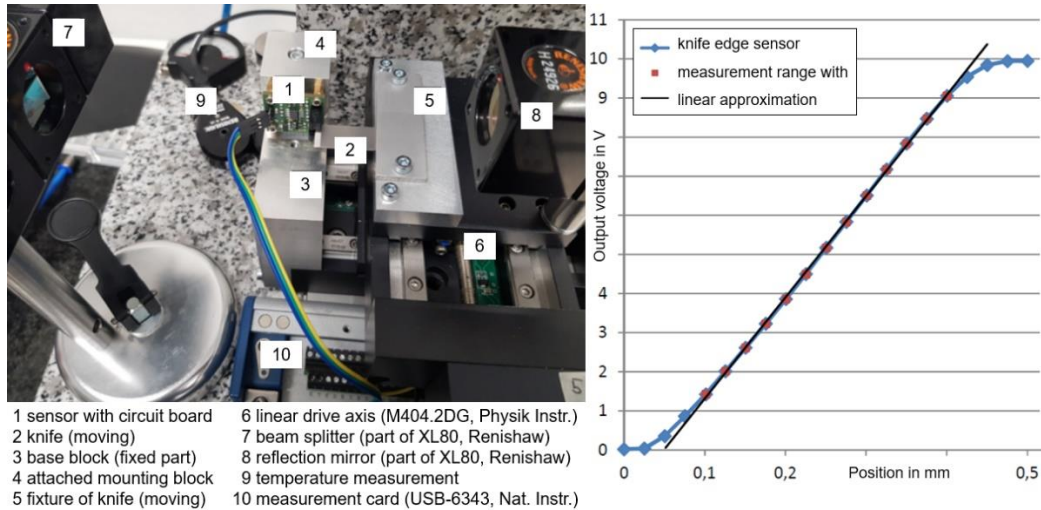


Fig. 4. Calibration setup for knife edge sensors with laser interferometer

The knife edge sensors were calibrated in a dedicated setup using a linear axis and laser interferometer (Renishaw XL80), see Fig. 4. These tests revealed a maximum measurement range of 500  $\mu\text{m}$ , a 300  $\mu\text{m}$  nearly linear measurement range, and a calibration coefficient of 26  $\text{mV}/\mu\text{m}$  in the linear range (Fig. 4). A motion reversal (backlash) error of 3.1  $\mu\text{m}$  and repeatability less than 1  $\mu\text{m}$  were also observed. Focusing on the 300  $\mu\text{m}$  linear measurement range ( $\pm 150 \mu\text{m}$ ), the dynamometer is intended to bear a static force of 5000 N (see Table 1) with a static deflection of 80  $\mu\text{m}$  and to sense proper values without any clipping of measurement signals or considerable nonlinearities.

### 3. VALIDATION

To validate the enhanced design of the dynamometer, two steps were required. First, the static and dynamic properties of the dynamometer were investigated. Second, machining tests were performed to illustrate the capabilities of the dynamometer and the applied evaluation methods.

#### 3.1. INVESTIGATION OF DYNAMIC PROPERTIES

The dynamic excitation was performed using both an impact hammer (250 gram hammer with Kistler 9721D500 force sensor) and an electromagnetic shaker. The response was measured by using the dynamometer's internal knife edge sensors as well as external

sensors for reference, see Fig. 5. Different force directions and locations were investigated. Considering linear modeling and dynamic superposition, the two perpendicular directions of X and Y proved to be sufficient for completing the scaling procedure.

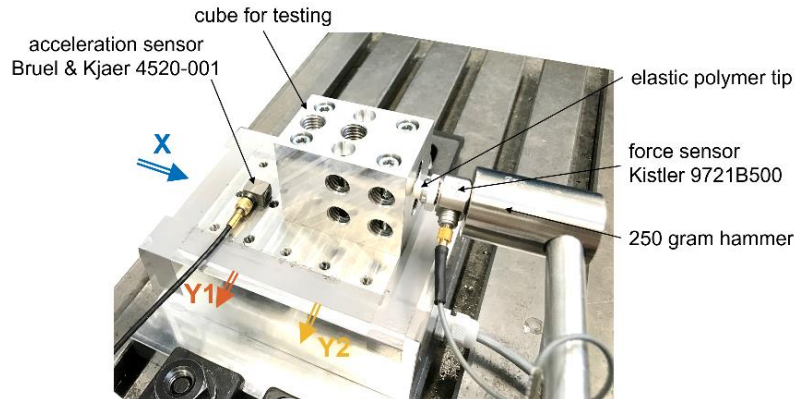


Fig. 5. FRF measurement with impact hammer force input; a cube was bolted to the moving platform to provide a target for force input

To seal the gap of the dynamometer against chips, flexible electrical tape was attached as a cover. The impact hammer tests and machining tests were both performed with the tape attached.

The voltage output signal of the individual knife edge sensors in relation to the aligned impact force was converted to the frequency domain and their ration was used to calculate the frequency response functions (FRFs, see Fig. 6). The translation modes in X and Y showed dominant natural frequencies slightly beneath 1,000 Hz. These natural modes reasonably agree with the simulated results, considering that the width of the flexure leaves was slightly decreased by deviations in the production process leading to decrease in natural frequency. When these FRFs are inverted and convolved with a Butterworth lowpass 4<sup>th</sup> order filter ( $f_{\text{corner}} = 1,300$  Hz) to attenuate high gains at high frequencies [20–23], they can be used as scaling functions to derive the force from the knife edge sensor voltage output.

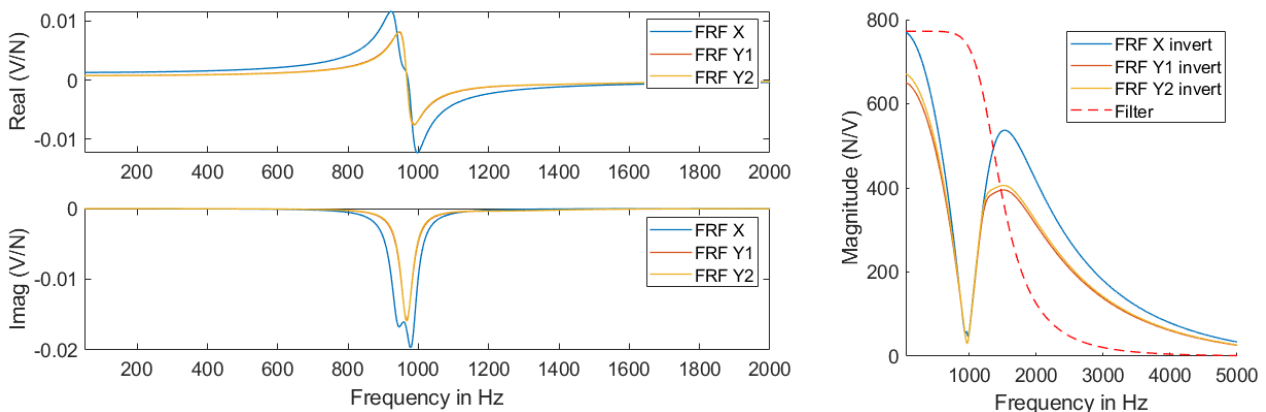


Fig. 6. left: Measured FRFs (sensor output to aligned force impact), right: Scaling functions and Butterworth lowpass filter

As shown in Fig. 1, the FRF of the knife edge sensor signals to the excitation force is measured. The measured FRF is fit using modal parameters and is inverted. This result is then multiplied by a lowpass filter since the inverted FRF tends to infinite amplitudes for frequencies above the resonance frequencies.

### 3.2. SETUP FOR MACHINING TESTS

The machining setup is displayed in Fig. 7. A 16 mm diameter screw-on milling head with two cutting inserts was used for machining aluminum EN-AW-6060 T66 along a straight path of 120 mm in a down-milling operation. The workpiece was bolted to the flexure-based dynamometer, however, the dynamometer was mounted to the table of a DMG Mori DMU 75 monoBLOCK. For reference measurement, a rotating dynamometer (Kistler 9170A) was used to record the forces as well. The tool was attached to a ground shaft which was clamped in the collet chuck of the rotating dynamometer. The total length from the HSK-63 spindle contact surface was 190.0 mm. Optical measurement (Zoller SmarTcheck 600) was used to accurately sense the radial position of the individual cutting edges, thus the radial misalignment affecting the uncut chip thickness of the individual cutting edge can be quantified.

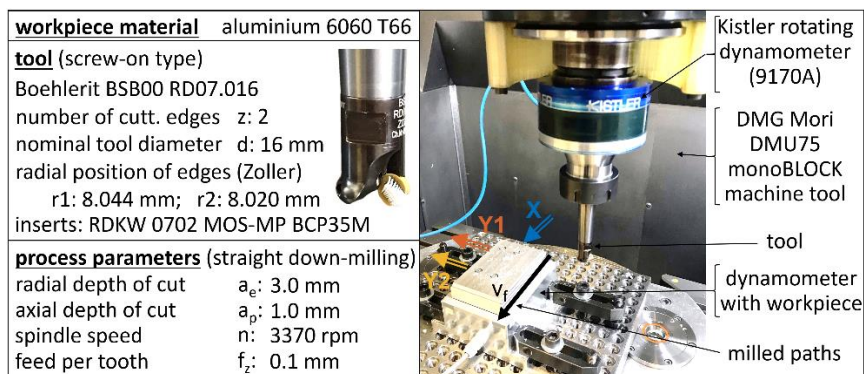


Fig. 7. Milling setup with flexure-based dynamometer and rotating dynamometer

Besides the initial setup shown in Fig. 7, the milling tool was changed to another kind of screw-on milling head and to a solid carbide tool. Moreover, spindle speed was varied and milled paths were chosen in  $Y$  direction for comprehensive testing of the dynamometer.

### 3.3. RESULTS AND DISCUSSION

Time domain voltages from both dynamometers were sampled at 19.2 kHz for signal analysis. The raw data (voltages) from the flexure-based dynamometer are presented in the top panel of Fig. 8. The results reveal an excitation of the structural modes by the cutting

force. This is clear for the feed ( $X$ ) direction, where high frequency oscillation is superimposed on the primary motion. In the time domain, the pattern repeats after one rotation, showing differences between the two cutting edges due to differences in radii (i.e., runout).

Applying the dynamic filtering allows to calculate the forces from displacement (voltage). The results in the middle panel of Fig. 8 depict the force in  $X$ -direction corresponding to the feed force  $F_f$  and the forces in the  $Y$ -direction represent the feed normal force  $F_{fN}$ . The bottom panel compares the dynamometer-based and rotating dynamometer active forces.

Since the Kistler rotating dynamometer senses in rotational frame of reference, a direct comparison of tool sided (Kistler) and workpiece sided (flexure-based dynamometer) measurements is not possible. However, the magnitude of both radial directions of tool sided measurement was calculated using Equation 1 and compared with the overall active force  $F_A$  of the flexure-base dynamometer (see bottom panel of Fig. 8).

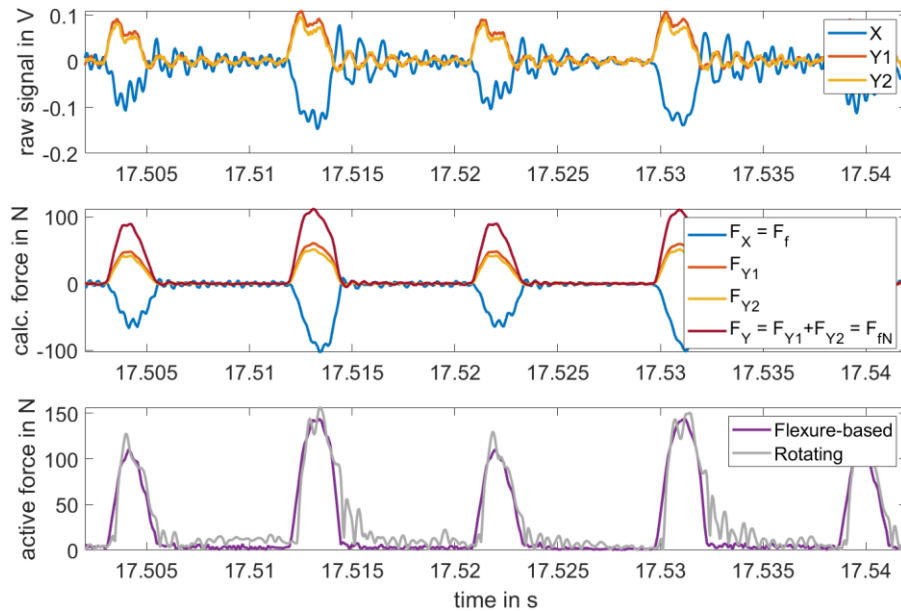


Fig. 8. Results of cutting tests

$$F_A^2 = F_f^2 + F_{fN}^2 = F_{r,x}^2 + F_{r,y}^2 \quad (1)$$

According to definition from DIN 6584 [24],  $F_A$  represents the active force,  $F_f$  the feed force,  $F_{fN}$  the feed normal force,  $F_{r,x}$  the radial force in  $X$ -direction of rotational dynamometer, and  $F_{r,y}$  the radial force in  $Y$ -direction of rotational dynamometer.

As the depth of cut was increased, chatter (or self-excited vibration) was observed in the dynamometer modes. As with any machining system, the spindle speed-depth of cut stability map can be derived and used to select stable machining conditions for force measurement [28]. The dynamometer design represents a compromise between a flexure-based structure that provides sufficient stiffness to enable reasonable machining conditions, but is not so stiff that the force resolution is too low.



## 4. CONCLUSION AND OUTLOOK

The concept of a single degree of freedom flexure-based dynamometer with low-cost sensors was enhanced by a new flexure-based design enabling a motion of the moving platform in three directions (two translations and one rotation). Consequently, three sensors were used to measure the platform motion. Impact hammer testing was applied to determine frequency domain scaling functions for the *X* and *Y* directions. These scaling functions were used to convert the measured displacement to the applied force. The displacements were measured using low-cost (optical) knife edge sensors. Finally, cutting experiments were used to compare the flexure-based dynamometer active force with a commercially available dynamometer. A good agreement between the two measurement results was observed.

In future work a mechanical design iteration will include a polymer seal for the gap between the moving mass and outer frame. This will protect against chips while also adding damping to increase the dynamometer's dynamic stiffness, which will increase the allowable chatter-free depth of cut.

Further investigations will include torque measurement (corresponding to *C*-axis) using this design of the flexure-based dynamometer. Additionally, automated procedures for tool wear tracking will be evaluated using the dynamometer sensitivity. Similar to integrated optical measurement routines for tool wear, offset correction in machining operations based on force information by integrated dynamometers can be used for determination of tool wear. Dedicated test cuts on machine table integrated dynamometers prior to machining a new workpiece may show potential for tracking tool condition periodically.

## ACKNOWLEDGEMENTS

*The authors want to express their appreciation and gratitude to the Austrian Marshall Plan Foundation for supporting the research work and strengthening the academic exchange between TU Wien and US universities. In addition, the authors dedicate a special mention and thanks to the Machine Tool Technologies Research Foundation (MTTRF) for the generous support of TU Wien, Institute of Production Engineering and Photonic Technologies.*

## REFERENCES

- [1] FLEISCHER J., DEUCHERT M., RUHS C., KÜHLEWEIN C., HALVADJIYSKY G., SCHMIDT C., 2008, *Design and Manufacturing of Micro Milling Tools*, *Microsyst. Technol.*, 14, 1771–1775.
- [2] DENKENA B., BIERMANN D., 2014, *Cutting Edge Geometries*, *CIRP Annals - Manufacturing Technology*, 63, 631–653.
- [3] BRECHER C., WECK M., 2017, *Werkzeugmaschinen Fertigungssysteme 2*, Springer-Verlag GmbH Berlin Heidelberg.
- [4] ABELE E., ALTINTAS Y., BRECHER C., 2010, *Machine Tool Spindle Units*, *CIRP Annals – Manufacturing Technology*, 59, 781–802.
- [5] KIENZLE O., 1954, *Einfluss der Wärmebehandlung von Stählen auf die Hauptschnittkraft beim Drehen*, *Stahl und Eisen*, 74, 530–551.
- [6] DENKENA B., TÖNSHOFF H.-K., 2010, *Spanen*, Springer-Verlag GmbH Berlin Heidelberg.
- [7] MICHELETTI G.F., KÖNIG W., VICTOR H.R., 1976, *In Process Tool Wear Sensors for Cutting Operations*, *CIRP Annals*, 25/2, 483–496.

- [8] BYRNE G., DORNFELD D., INASAKI I., KETTELER G., KÖNIG W., TETI R., 1995, *Tool Condition Monitoring (TCM) — The Status of Research and Industrial Application*, CIRP Annals, 44/2, 541–567.
- [9] TETI R., JEMIELNIAK K., O'DONNELL G., DORNFELD G., 2010, *Advanced Monitoring of Machining Operations*, CIRP Annals – Manufacturing Technology, 59, 717–739.
- [10] WYEN C.-F., WEGENER K., 2010, *Influence of Cutting Edge Radius on Cutting Forces in Machining Titanium*, CIRP Annals – Manufacturing Technology, 59, 93–96.
- [11] MEDYK P., KASPRZAK M., 2020, *Approach to Feed Drive Load Measurements in Heavy Turning*, Journal of Machine Engineering, 20/4, 41–58.
- [12] KASPRZAK M., PYZALSKI M., 2021, *Testing of Force Sensors for the Active Measurement and Limitation of Axial Loads in Heavy Turning*, Journal of Machine Engineering, 21/4, 106–117.
- [13] AGGARWAL S., NESIC N., XIROUCHAKIS P., 2013, *Cutting Torque and Tangential Cutting Force Coefficient Identification from Spindle Motor Current*, Internat. Journal of Advanced Manufacturing Techn., 65, 81–95.
- [14] XU X., ZHANG Y., LI Y., LI Y., 2022, *Machine Learning Cutting Forces in Milling Processes of Functionally Graded Materials*, Advances in Computational Intelligence (ADCI), 2, 25.
- [15] TETI R., MOURTZIS D., D'ADDONA D., CAGGIANO A., 2022, *Process Monitoring of Machining*. CIRP Annals, 71/2, 529–552.
- [16] BLEICHER F., BIERMANN D., DROSSEL W., MÖHRING H.-C., ALTINTAS Y., Forthcoming 2023, *Sensor and Actuator Integrated Tooling Systems*, CIRP Annals.
- [17] DENKENA B., DAHLMANN D., BOUJNAH H., 2016, *Sensory Workpieces for Process Monitoring –an Approach*, Procedia Technology, 26, 129–135.
- [18] DENKENA B., DAHLMANN D., KIESNER J., 2016, *Production Monitoring Based on Sensing Clamping Elements*, Procedia Technology, 26, 235–244.
- [19] PALALIC M., MÖHRING H.-C., MAIER W., MENDOZA A., RIEMEIER F., 2020, *Multiaxial Force Platform with Disturbance Compensation for Machine Tools*, Journal of Machine Engineering, 20/3, 5–16.
- [20] GOMEZ M., SCHMITZ T., 2019, *Displacement-Based Dynamometer for Milling Force Measurement*, Procedia Manufacturing, 34, 867–875.
- [21] GOMEZ M., SCHMITZ T., 2020, *Low-cost, Constrained-Motion Dynamometer for Milling Force Measurement*, Manufacturing Letters, 25, 34–39.
- [22] GOMEZ M., HONEYCUTT A., SCHMITZ T., 2021, *Hybrid Manufactured Dynamometer for Cutting Force Measurement*, Manufacturing Letters, 29, 65–69.
- [23] GOMEZ M., SCHMITZ T., 2022, *Stability Evaluation for a Damped, Constrained-motion Cutting Force Dynamometer*, Journal of Manufacturing and Materials Processing, 6/1, 23, 1–26.
- [24] Deutsches Institut für Normung e.V., 1982, *DIN 6584-5 - Begriffe der Zerspantechnik - Kräfte Energie Arbeit Leistungen*, Berlin.
- [25] RUBEO M., SCHMITZ T., 2016, *Mechanistic Force Model Coefficients: A Comparison of Linear Regression and Nonlinear Optimization*, Journal of the International Societies for Precision Engineering and Nanotechnology, 45, 311–321.
- [26] KORKMAZ E., GOZEN B.A., BEDIZ B., OZDOGANLAR O.B., 2017, *Accurate Measurement of Micromachining Forces Through Dynamic Compensation of Dynamometers*, Journal of the International Societies for Precision Engineering and Nanotechnology, 49, 356–376.
- [27] ZAMEROSKI R., GOMEZ M., SCHMITZ T., 2022, *Geometry-Based, Gaussian Profile Model for Optical Knife-Edge Displacement Sensor*, Precision Engineering, 73, 470–476.
- [28] SCHMITZ T., SMITH S., 2019, *Machining Dynamics: Frequency Response to Improved Productivity*, Second Edition, Springer, New York, NY.